Lifetime measurements of the $7D$ levels of atomic francium

J. M. Grossman,* R. P. Fliller III, L. A. Orozco, M. R. Pearson, and G. D. Sprouse
Department of Physics and Astronomy, State University of New York, Stony Brook, New York 11794-3800
(Received 21 June 2000; published 30 October 2000)

We present lifetime measurements of the $7D_{3/2}$ and $7D_{5/2}$ levels of Fr. We use a time-correlated single-photon counting technique on a sample of ^{210}Fr atoms confined and cooled in a magneto-optical trap. The upper state of the $7P_{3/2}$ trapping transition serves as the resonant intermediate level for two-photon excitation of the $7D$ states. A probe laser provides the second step of the excitation, and we detect the decay of the atomic fluorescence. Our measurements help extend the knowledge of this class of atomic wave functions in which correlation effects are very significant. We measure lifetimes of 73.6 ± 0.3 ns and 67.7 ± 2.9 ns for the $7D_{3/2}$ and $7D_{5/2}$ levels, respectively.

PACS number(s): 32.70.Cs, 31.15.Ar, 32.80.Pj

I. INTRODUCTION

The wealth of work performed on francium at ISOLDE [1] opened the possibility to cool and trap this radioactive heavy alkali metal in sufficient quantities to perform further spectroscopic studies [2,3]. Until now, our experimental work on the electronic states of francium has been on the low-lying S and P states. (See Refs. [4–6], for example.) The understanding of these states—their energies, dipole matrix elements, and hyperfine constants—is beginning to reach a level comparable to that of the other alkali metals. Of particular interest is the quantitative knowledge reached by the atomic theory calculations [7–9] and its agreement with our measurements, strengthening the possibility of a parity nonconservation (PNC) measurement in a chain of francium isotopes [10].

We would like to reach a similar quantitative understanding of the low-lying $7d$ level. To this end, we are performing accurate measurements of properties of the levels that give us information about the quality of the theoretical calculations both at short range (hyperfine structure) and at long range (atomic lifetimes). The energies and hyperfine structure of high-lying D states ($n=8-20$) have been measured previously [1,11]. We recently located the energies and measured the hyperfine structure of the $7D_{3/2}$ and $7D_{5/2}$ states [12]. The very different angular momentum properties of the d levels, particularly the large contributions from correlation corrections, make calculations of their structure from first principles more complicated than for the s and p levels. Fortson [13] has a scheme to perform a PNC measurement in Ba^+, using the $6S$ and $5D$ states by monitoring the ground-state spin rotation induced by an intense laser beam. Although it is not possible to directly adapt this suggestion to a measurement in Fr using the $7S$ and $6D$ levels, other schemes may be feasible and require further study.

In this paper we report measurements of the lifetime of the $7D_{3/2}$ and $7D_{5/2}$ states that present a new challenge to the most sophisticated techniques of *ab initio* calculations using many-body perturbation theory (MBPT). The structure of the paper is as follows. Section II reviews how we make, capture, and probe Fr. Section III explains our use of a time-correlated single-photon counting method as applied to a small sample of trapped and cooled Fr atoms. We present our measurements in Sec. IV, with a discussion of them in Sec. V. Section VI summarizes our results and we conclude with Sec. VII.

II. PREPARATION OF SAMPLE

The production, cooling, and trapping of Fr on line with the Superconducting LINAC at Stony Brook have been described previously [14]. Briefly, to make Fr, a 100-MeV beam of ^{18}O ions from the accelerator impinges on a gold target. We extract $\sim 1 \times 10^6$ francium ions/s out of the gold and transport them about 1 m to a hot (~ 1000 K) yttrium neutralizer. From here the neutral atoms enter a dry-film coated glass cell where they are cooled and trapped in a magneto-optical trap (MOT) with $10^3 - 10^4$ atoms captured in steady state. The trap operates on line in the target room of the accelerator with the experiment controlled remotely.

Figure 1 shows the energy levels of ^{210}Fr relevant for trapping and the lifetime measurements. A Coherent 899-21 titanium-sapphire laser operating at 718 nm excites the trapping and cooling transition ($7S_{1/2}, F=\frac{13}{2} \rightarrow 7P_{3/2}, F=\frac{15}{2}$). An EOSI 2010 diode laser operating at 817 nm repumps any atoms that leak out of the cooling cycle via the $7S_{1/2}, F=\frac{11}{2} \rightarrow 7P_{1/2}, F=\frac{13}{2}$ transition. A computer-controlled scanning Fabry-Perot cavity monitors and holds the long-term frequencies of both lasers [19]. A charge-coupled-device (CCD) camera collects the trapping cycle fluorescence and monitors the number of atoms in the trap during measurements.

We operate in a regime where the steady-state number of atoms is small, a few thousand, to make sure that the density of the sample is low (trap diameter 1 mm). The trap operates with a typical detuning of 4Γ, where $\Gamma = 1/\tau$ and an intensity that produces a generalized Rabi frequency of $\sim 4.5\Gamma$ [12].

III. METHOD AND APPARATUS

We measure the lifetime of the $7d$ levels using time-correlated single-photon counting [15]. This method has been used, for example, to measure lifetimes of atoms in

*Electronic address: Joshua.Grossman@sunysb.edu

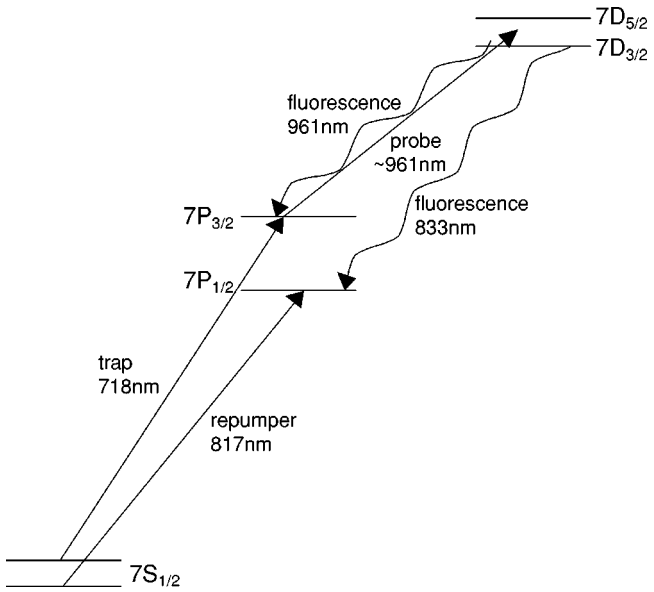

FIG. 1. Energy levels and lasers relevant to the trap operation and lifetime measurements.

beams [16], atoms in vapor cells [17], and trapped single ions [18]. We applied it for the lifetime measurements of the $7p$ levels of trapped atomic francium [4].

The time-correlated single-photon counting uses a short pulse of resonant laser light to populate an excited state at $t=0$. The arrival times, with respect to the excitation pulse, of the spontaneously emitted photons when histogrammed directly show the exponential decay of the state. The technique requires some care to have a small enough excitation rate in order to minimize systematic problems from pulse pileup. It works best with thin samples of atoms and we operate in a regime where the likelihood of getting a fluorescence photon per excitation is much less than 1 [4]. Roughly, the fractional statistical inaccuracy of the method scales with $1/\sqrt{N}$, where N is the number of detected photons [18]. So it is possible to achieve accuracies of a fraction of 1%.

We have adapted the technique that we applied to the $7p$ levels to measure the $7d$ levels. We require a two-photon transition to excite the $7d$ levels. The resonant intermediate level is the upper state of the trapping transition, $7P_{3/2}$, $F=\frac{15}{2}$. A second Coherent 899-21 titanium sapphire laser operating at 969 nm or 961 nm excites the transition from the intermediate level to the recently observed $7D_{3/2}$, $F=\frac{15}{2}$ or $7D_{5/2}$, $F=\frac{17}{2}$ levels [12], respectively. A Burleigh WA-1500 wavemeter measures the frequencies of all three lasers. Figure 2 shows a block diagram of the experimental system.

The measurement operates on a 1-μs cycle, as shown in Fig. 3. We keep the trapping and cooling lasers on all the time, then we excite a small fraction of the atoms in the $7P_{3/2}$ state with the 969-nm or 961-nm probe laser. Following the probe pulse, we detect the decay of fluorescence for 500 ns.

The probe laser is chopped by two Gsänger LM0202 electro-optic modulators (EOMs). We use two modulators to extinguish the light as sharply and thoroughly as possible. The extinction ratio is better than 150:1 (after 30 ns). This

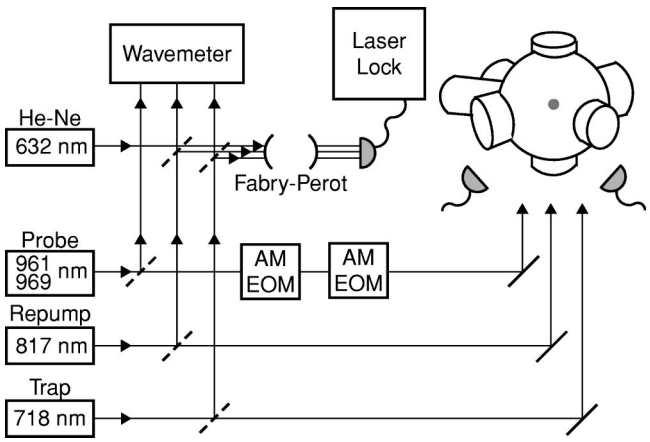

FIG. 2. Block diagram of experiment.

less than optimal performance comes from the large wavelength of the excitation, 35% longer than the designed wavelength for the EOMs. The probe laser is on for 200 ns each cycle.

An $f/1.3$ optical system collects the fluorescence. A 1-mm-diam aperture at a focal point in the assembly rejects light spatially separated from the trapped atoms. This reduces the background and prevents saturation of the photomultiplier tube (PMT). For the measurement of the $7D_{3/2}$ lifetime, a Hamamatsu R636-10 PMT operating in photon-counting mode detects the 833-nm fluorescence of the decay from the $7D_{3/2}\rightarrow 7P_{1/2}$ level. Appropriate glass and interference filters reject light at other wavelengths. Because the $7D_{5/2}$ level does not decay to the $7P_{1/2}$ level, a cooled Hamamatsu R2658P PMT with appropriate interference filters detects the 961-nm fluorescence of the decay from the $7D_{5/2}\rightarrow 7P_{3/2}$ level. The quantum efficiency of this PMT ($\sim$0.3% at 961 nm) is more than an order of magnitude lower than that of the R636-10 ($\sim$7% at 833 nm). At this wavelength, scattered blackbody radiation from sources such as the nearby hot neutralizer cannot be completely excluded.

We amplify and discriminate the pulses from the PMT

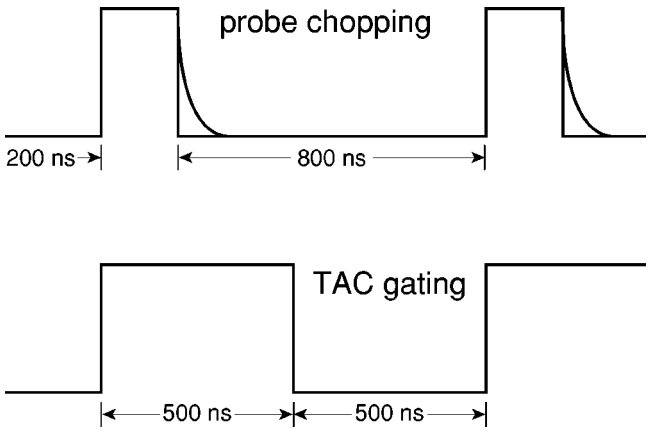

FIG. 3. Timing for the lifetime measurements. The upper trace is the chopping of the probe with the decay of the fluorescence from the $7D_J$ state indicated schematically. The lower trace is the TAC gating.

before sending them to the pulse processing electronics. We keep the rate of photon counts low to prevent double pulse events and reduce dead-time systematic effects in the electronics.

The timing sequence for the chopping and detection is derived from a BNC 8010 pulse generator triggering two LeCroy 222 gate and delay generators. Detected fluorescence photon-counting pulses start an Ortec 467 time-to-amplitude converter (TAC), and the TAC stop pulse comes from one of the gate generators. Starting the TAC with a fluorescence photon eliminates the accumulation of counts from cycles with no detected photons. A multichannel analyzer (MCA) bins the TAC output to produce a histogram of the events.

The Gsänger EOMs extinguish the probe light in a finite time. The turn-off function is well modeled by a Gaussian, so we describe the fluorescence function as the convolution of a Gaussian with an exponential decay. In our measurements of the $7D_{5/2}$ lifetime, the PMT counts photons at the excitation wavelength, so scattered photons from the excitation pulse are also counted.

IV. MEASUREMENTS AND FITS

We accumulate $\sim$1000 fluorescence counts/channel in 2048 channels for the $7D_{3/2}$ lifetime and $\sim$30 counts/channel in 8192 channels for the $7D_{5/2}$ lifetime in about 30 min per data set with atoms in the trap and the probe laser on resonance. The signal gives the exponential decay of the fluorescence for about five lifetimes for the $7D_{3/2}$ measurement and about three lifetimes for the $7D_{5/2}$ measurement. The statistical quality of the data is much better for the $7D_{3/2}$ lifetime measurements, than for the $7D_{5/2}$ measurements. For the $7D_{3/2}$ measurement, the background count rate is 1500 Hz, mostly from scattered light from the trap laser that leaks through the interference filter. For the $7D_{5/2}$ lifetime measurement (961-nm photon counting), the background count rate is 600 Hz mostly from blackbody radiation of the hot neutralizer, from dark counts, and from the trap laser. We also shift the trap laser off resonance so that there are no atoms in the trap and collect background to look for systematic effects in the timing electronics.

The chopping EOMs have a finite switching time. To study the excitation pulse, we collect background data by counting photons scattered from the probe pulse without any atoms in the trap. The pulse is well modeled by a flat top with a half-Gaussian turn-on and turn-off. Taking time t as the independent variable, we fit to the function

$$f(t)=\begin{cases} Ae^{-(t-t_c+d)^2/(2w^2)}, & t-t_c\leqslant -d \\ A, & |t-t_c|<d \\ Ae^{-(t-t_c-d)^2/(2w^2)}, & t-t_c\geqslant d \end{cases} \tag{1}$$

and obtain the pulse center t_c, the pulse width $2d$, and the switching time constant w. For a population of atoms starting at $t=0$ in the $7D_J$ state, the excited-state population decay is given by

$$g(t)=\begin{cases} 0, & t<0 \\ Be^{-t/\tau}, & t\geqslant 0, \end{cases} \tag{2}$$

where τ is the $7D_J$ state lifetime. After the start of the pulse turn-off, the fluorescence decay is given by the convolution of f and g,

$$(f\circ g)(t)=\int_{-\infty}^{t} f(T)g(t-T)dT. \tag{3}$$

We operate with probe intensities well below the two-level saturation intensity of 3.1 mW/cm^2. In our experiment the probe pulse is sufficiently long ($\sim$200 ns) that we can neglect the pulse turn-on [the first line of Eq. (1)]. Doing this and substituting Eqs. (1) and (2) into Eq. (3) yields

$$\begin{aligned}(f\circ g)(t)=A'\Bigg\{ & \tau e^{-t/\tau}(e^{(d+t_c)/\tau}-e^{(-d+t_c)/\tau}) \\ & +\frac{\sqrt{2\pi}}{2w}e^{-(2t\tau-2d\tau-2t_c\tau-w^2)/\tau^2}\Bigg[\operatorname{erf}\left(\frac{w\tau}{\sqrt{2}\tau}\right) \\ & +\operatorname{erf}\left(\frac{t\tau-d\tau-t_c\tau-w^2}{\sqrt{2}w\tau}\right)\Bigg]\Bigg\}, \end{aligned} \tag{4}$$

where $A'=AB$ and $\operatorname{erf}(x)$ is the error function. The first term in Eq. (4) is just a pure exponential decay resulting from the flat part of the pulse. The second term results from the finite turn-off. In the limit of infinitely fast switching ($w\rightarrow 0$), Eq. (4) reduces to a pure exponential decay.

Our measurements of the $7D_{3/2}$ lifetime count photons at a different wavelength from the probe laser, so the PMT does not count scattered photons from the probe pulse. We fit these data sets with

$$h_{3/2}(t)=(f\circ g)(t)+c, \tag{5}$$

where c is a constant background. The fit takes values of w, d, and t_c obtained from background data sets and uses A', τ, and c as free parameters. Results obtained in this way agree with the results of fits to a region well after the probe turn-off, using a pure exponential decay plus a constant background. We report the results of the latter fits as they involve fewer parameters. Figure 4 shows an example $7D_{3/2}$ decay curve data set with an exponential fit.

For the $7D_{5/2}$ lifetime measurements, the detection wavelength is the same as the excitation wavelength, so the PMT also counts scattered photons from the probe pulse. We fit these data sets with

$$h_{5/2}(t)=(f\circ g)(t)+f(t)+c, \tag{6}$$

The fit takes A, A', τ, and c as free parameters, and w, d, and t_c are fixed from background data fits. This approach allows us to include sections of the data in which the atomic fluorescence has not decayed much. In these sections the signal-to-noise ratio is much greater than in sections well after the probe turn-off, where counted photons are nearly a pure exponential decay. Figure 5 shows a sample $7D_{5/2}$ decay data

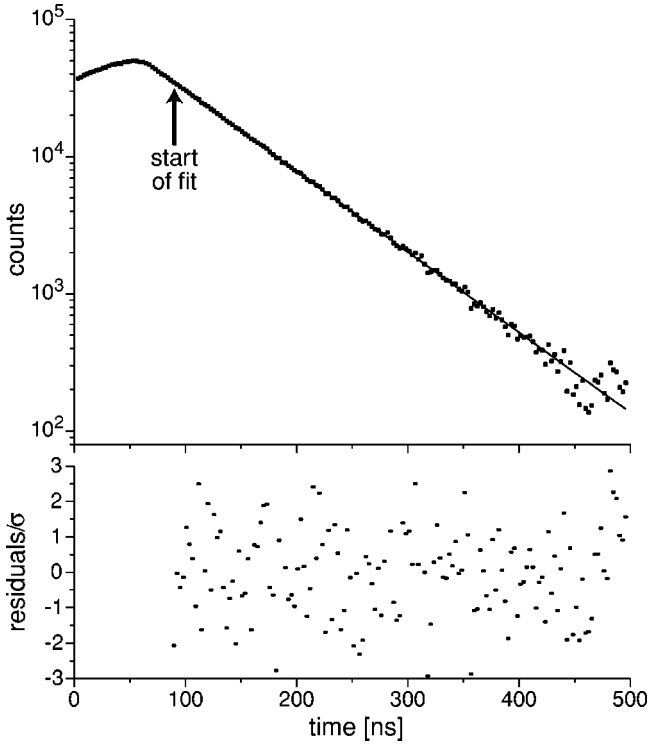

FIG. 4. Decay curve of the $7D_{3/2}$ level with fit residuals. On the upper plot the data points are the fluorescence counts minus a constant background. (Every ten channels have been added together.) The line is a fit to an exponential decay. The lower plot shows the residuals of the fit divided by the statistical uncertainty of each point.

set with the corresponding fits. The solid line is a fit to data using Eq. (6). The dashed line is a scaled fit of Eq. (1) to a background data set collected by counting photons while applying the excitation pulses with no atoms in the trap.

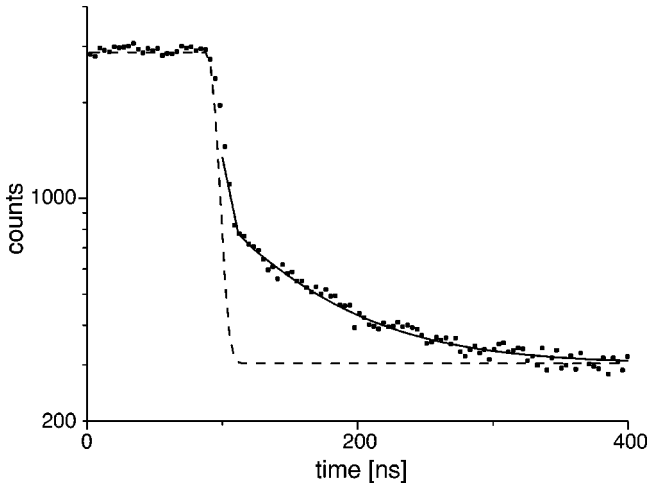

FIG. 5. Decay curve of the $7D_{5/2}$ level. The data points are the fluorescence counts from the excitation pulse and the subsequent decay of the $7D_{5/2} \rightarrow 7P_{3/2}$ fluorescence. (Every 20 channels have been binned together.) The solid line is a fit to the data and the dashed line is a scaled fit to a background data set as explained in the text.

V. DISCUSSION

We calibrate the time scale of the TAC and MCA with a 9.5-MHz oscillator with a stability better than 1×10^{-6}. An unchopped laser produces photon counts, which we gate with the oscillator. The gated pulses serve as both the start and stop of the TAC. This produces randomly distributed events separated in time by an integer number of periods of the oscillator. The time calibration of the TAC and MCA has an uncertainty of $\pm0.04\%$ and $\pm0.06\%$ for the $7D_{3/2}$ and $7D_{5/2}$ measurements, respectively. For both measurements the time scale is linear to $\pm0.04\%$ over the entire range of channels with data. Fitting the lifetime measurements with a time scale that is linear with an adjustable quadratic correction has a negligible effect on the lifetimes. We measure the linearity in the height scale of the TAC and MCA with photons from a flashlight source that are randomly separated in time. The binned counts are entirely consistent with a flat line.

For a given cycle, the TAC can only register one photon. A correction to the raw data accounts for the preferential counting of early events [15]. If N_i is the number of counts in MCA channel i, and n_E is the total number of excitation cycles, then N_i', the corrected number of counts in channel i, is given by

$$N_i' = \frac{N_i}{1-\frac{1}{n_E}\sum_{j<i} N_j}. \tag{7}$$

Low count rates, as in our case, keep this correction small. The correction alters the fitted lifetime of the $7D_{3/2}$ state by 0.06%. It does not significantly affect the fitted lifetime of the $7D_{5/2}$ state because of the low statistics of the measurement.

Adjusting the range over which the data are fitted, we find a variation in the obtained lifetime. We change the beginning and end of each data range and find no systematic trends in the fluctuation of the lifetimes. The truncation uncertainty is the standard deviation of the lifetime for different starting and ending points of the fit. For the $7D_{3/2}$ measurement, the uncertainty is $\pm0.11\%$, and for the $7D_{5/2}$ measurement an uncertainty of $\pm1.03\%$ accounts for the variation.

We have searched for quantum beats in the fluorescence decay signal but have not observed any. Quantum beats arise when a short laser pulse excites two closely spaced energy levels with energies E_1 and E_2 from a common lower level. To coherently excite the two levels with a laser pulse, the spectral bandwidth of the pulse must be greater than the frequency separation of the levels. The quantum interference between the levels then modulates the total exponential decay of the fluorescence. Following the treatment of Demtröder [20], the total intensity of the emitted fluorescence with quantum beats as a function of time is

$$I(t) = Ce^{-t/\tau}\,[D + E\cos(\omega_{21}t)], \tag{8}$$

where $\omega_{21}=(E_2-E_1)/\hbar$. The coefficients D and E can be computed from the matrix elements between the levels involved in the excitation and decay transitions. The excitation

and fluorescence geometries also determine the spatial dependence of the amplitude of the quantum beats E.

In ^{210}Fr, the adjacent hyperfine level is separated by 167 MHz for the $7D_{3/2}$ state and 117.5 MHz for the $7D_{5/2}$ state [12]. This is much larger than the $\leqslant 500$ kHz bandwidth of the exciting laser. The 30-ns turn-off time of the chopping EOMs is too long to give sufficient laser bandwidth to coherently excite both hyperfine states. A fast Fourier transform of the fit residuals reveals no distinguishable components at the hyperfine splitting frequency.

The $7D_J$ hyperfine levels that we excite also have magnetic sublevels that can potentially contribute quantum beats. If the Zeeman quantum beats have a period of oscillation longer than the atomic lifetime, they could cause a systematic shift in the lifetime. A magnetic field shifts a hyperfine magnetic sublevel m_F in energy by $\Delta E = g_F \mu_B B m_F$, where g_F is the g factor for the level, μ_B is the Bohr magneton, and B is the external magnetic field. The difference in energy shifts between sublevels determines the beat frequency. The MOT requires a magnetic-field gradient in three dimensions that is present during the measurements. The atoms at different locations in the trap experience different energy shifts. For balanced MOT beam intensities and polarizations, the trap center is at the zero of the magnetic field. The different energy shifts due to the MOT magnetic-field gradient, together with the different light polarizations resulting from the intersection of the three pairs of σ_+- and σ_-- polarized laser beams, tend to average out the effect of Zeeman beats.

We have calculated the maximum contribution of the Zeeman quantum beats to the fitted lifetimes. Following Ref. [21], for a rectangular excitation pulse $P(t_e)$ of length θ and a detection window of width δ occurring at time Δt after the center of the excitation pulse, the rate of fluorescence is given by

$$R(\Delta t,\theta,\delta) \propto \sum_{m,m',\mu,\mu'} f_{\mu m} f_{m\mu'} g_{\mu' m'} g_{m'\mu} \times \int_{\Delta t+\delta/2}^{\Delta t+\delta/2} \int_{\theta/2}^{\theta/2} P(t_e) \times \exp[-(i\omega_{\mu\mu'}+\Gamma)(t'-t_e)]dt_e dt', \quad (9)$$

where f and g are, respectively, the excitation and decay transition matrix elements connecting the lower states m and m' with the upper states μ and μ'. The decay rate is $\Gamma = 1/\tau$ and $\omega_{\mu\mu'} = (E_\mu - E_{\mu'})/\hbar$. Integrating, we find

$$\begin{aligned} R(\Delta t,\theta,\delta) \propto & \sum_{m,m',\mu,\mu'} f_{\mu m} f_{m\mu'} g_{\mu' m'} g_{m'\mu} \\ & \times [e^{-\Gamma T}/(\Gamma^2+\omega^2)^2] \\ & \times \{[\omega^2-\Gamma^2+2i\omega\Gamma][\cos\omega T + e^{-\Gamma\Theta} \\ & \times \cos\omega(T+\Theta) - e^{-\Gamma\theta}\cos\omega(T+\theta) \\ & - e^{-\Gamma\delta}\cos\omega(T+\delta)] + [2\omega\Gamma - i(\omega^2-\Gamma^2)] \\ & \times [\sin\omega T + e^{-\Gamma\Theta}\sin\omega(T+\Theta) - e^{-\Gamma\theta} \\ & \times \sin\omega(T+\theta) - e^{-\Gamma\delta}\sin\omega(T+\delta)]\}, \end{aligned} \quad (10)$$

where $\Theta = \theta + \delta$ and $T = \Delta t - \Theta/2$. In the limit of a long excitation pulse, the terms involving θ are negligible. The width of the MCA bins corresponds to $\delta = 0.2784$ ns and $\delta = 0.1776$ ns for the $7D_{3/2}$ and $7D_{5/2}$ measurements, respectively. Our excitation and detection geometry allows coherences between excited m_F sublevels differing by $\Delta m_F = 2$ [21]. If a 1-mm trap forms at the zero of the field in the 6-G/cm gradient, the expected beat frequency for atoms at the maximum field of 0.3 G is 134 kHz for $7D_{3/2}, F = \frac{15}{2}$ and 296 kHz for $7D_{5/2}, F = \frac{17}{2}$. In our calculations, the quantum beats affect the lifetime measurement negligibly.

TABLE I. Error budget for the lifetime measurements.

Error	$7D_{3/2}$ (%)	$7D_{5/2}$ (%)
Statistical	± 0.38	± 4.14
Truncation	± 0.11	± 1.03
Time calibration	± 0.04	± 0.06
TAC/MCA nonlinearity	$< \pm 0.01$	$< \pm 0.01$
Quantum beats	$< \pm 0.01$	$< \pm 0.01$
Total	$\pm$ **0.40**	$\pm$ **4.3**

The intense trap laser creates an Autler-Townes (ac Stark) splitting of the intermediate $7P_{3/2}, F = \frac{15}{2}$ state [12]. This splitting is typically ~ 35 MHz. Numerical optical Bloch equation calculations of the evolution of the level populations and coherences indicate no discernible effect on the measured lifetime from this splitting.

The density of the atoms in the trap is low (10^3–10^4 atoms in 1 mm^3). In this regime, effects such as radiation trapping, superfluorescence, and quenching due to collisions do not alter the measured lifetime. In our previous measurements [4] of the lifetimes of the $7P$ states in Fr and the $5P$ states in Rb, we studied several other possible sources of error that contribute at a level that is negligible in the measurements reported here. An imbalance of the trap laser beams that displaces the trap center by one trap diameter (~ 1 mm) does not significantly affect the measured lifetime through Zeeman quantum beats or any other means. Varying the MOT magnetic-field gradient does not affect the measurements. The number of atoms in the trap is small so that any residual probe laser light that is not fully extinguished by the chopping EOMs does not cause a measurable background count rate. Modulation of the trap laser frequency also affects the obtained values at a level that is negligible in these measurements.

TABLE II. Comparison of measured lifetimes with theoretical predictions from semiempirical calculations and *ab initio* MBPT calculations of radial matrix elements.

	$\tau(7D_{3/2})$(ns)	$\tau(7D_{5/2})$(ns)
This work [$\tau(7D_J)$]	**73.6** $\pm$ **0.3**	**67.7** $\pm$ **2.9**
Dzuba *et al.* [7]	75.4	68.7
Safronova and Johnson [9]	76.0	69.5
van Wijngaarden and Xia [22]	75.9	70.3
Biémont *et al.* [23]	53	77
Theodosiou [24]	74.5	82.7

TABLE III. Elements of Table IV of [7], radial integrals for Fr (in units of the Bohr radius). The $7s$-$7p_{J_k}$ radial integral calculations converge much better than the $7p_{J_i}$-$7d_{J_k}$ integral calculations.

Transition	RHF	TDHF	Brueckner orbitals	Brueckner plus non-Brueckner	Prediction
$7s$-$7p_{1/2}$	−6.311	−5.851	−5.261	−5.241	−5.271
$7s$-$7p_{3/2}$	−6.153	−5.742	−5.124	−5.104	−5.133
$7p_{1/2}$-$7d_{3/2}$	−1.722	−1.855	−3.015		
$7p_{3/2}$-$7d_{3/2}$	−2.670	−2.791	−4.213		
$7p_{3/2}$-$7d_{5/2}$	−2.759	−2.850	−3.992		

VI. RESULTS

Table I contains the error budget for the lifetime measurements. The standard deviation of the mean of the lifetime fits is $\pm 0.38\%$ for the $7D_{3/2}$ state and $\pm 4.14\%$ for the $7D_{5/2}$ state. Combining the uncertainties in quadrature gives a total uncertainty of $\pm 0.40\%$ and $\pm 4.3\%$, respectively. This gives lifetime results of 73.6 ± 0.3 ns for the $7D_{3/2}$ state and 67.7 ± 2.9 ns for the $7D_{5/2}$ state.

Table II compares our lifetime measurement results with predictions based on semiempirical calculations of oscillator strengths [22,23] and radial matrix elements [24], and with lifetimes obtained from radial matrix elements calculated by *ab initio* many-body perturbation theory [7,9]. The lifetime of an excited state k is related to the decay rates to other states i by

$$\frac{1}{\tau_k} = \sum_i \frac{1}{\tau_{k \to i}}. \tag{11}$$

The decay rate to a state i is related to the reduced radial matrix element between the two states by

$$\frac{1}{\tau_{k \to i}} = \frac{4}{3} \frac{\omega_{ki}^3}{c^2} \alpha \frac{|\langle J_i \| \mathbf{r} \| J_k \rangle|^2}{2J_k + 1}, \tag{12}$$

where ω_{ki} is the transition energy divided by $\hbar$, c is the speed of light, α is the fine-structure constant, J_i is the angular momentum of state i, and $\langle J_i \| \mathbf{r} \| J_k \rangle$ is the reduced matrix element. [Note that Dzuba *et al.* calculate the radial integral $\int R_i(r) r R_k(r) dr$. To obtain the radial matrix element $\langle J_i \| \mathbf{r} \| J_k \rangle$, multiply the radial integral by the angular coefficient $\langle J_i \| \hat{\mathbf{r}} \| J_k \rangle$.] Because we measure the lifetimes of the $7D$ states but not the branching ratios of their decay, we cannot obtain the radial matrix elements from our results. We can, however, use the *ab initio* and semiempirical calculations of radial matrix elements to obtain predictions for the lifetimes to compare with our results.

The $7D_{3/2}$ state can decay to the $7P_J$ and $8P_J$ ($J = \frac{1}{2}, \frac{3}{2}$) states, and the $7D_{5/2}$ state decays to the $7P_{3/2}$ and $8P_{3/2}$ states. Because the energies of the $8P_J$ states [25] are so close to that of the $7D_J$, they contribute less than 1% to the total decay rate. As a result, they have been neglected in the calculations of [7,9,23]. The level of agreement obtained by the *ab initio* calculations of Dzuba *et al.* [7] and Safronova and Johnson [9] is impressive given the complexity of the calculations. Still, the agreement of calculations [7,8] with previous measurements of the $7P_J$ lifetimes is about a factor of 2 better than here. (The calculated $7P_J \to 7S_{1/2}$ matrix elements agree within 1% with the experimentally derived values.) The large contributions from core electron correlations associated with the D states are the main factor limiting the precision of atomic calculations for these states [9,26]. Table III reproduces elements of Table IV of Ref. [7]. The $7P_{1/2,3/2} \to 7S_{1/2}$ calculations clearly seem to be converging with each successive correction smaller than the previous one. On the other hand, the $7D_{3/2,5/2} \to 7P_{1/2,3/2}$ do not appear to be converging. With large correlation corrections, the D states are not as well suited to perturbative treatment as are the S and P states.

VII. CONCLUSION

We have used two-photon excitation and time-correlated single-photon counting techniques on a sample of cold ^{210}Fr atoms confined in a MOT to measure the lifetimes of the $7D_{3/2}$ and $7D_{5/2}$ excited states. These lifetimes are the first test of calculations of radial matrix elements connecting two excited states in Fr. They provide a more stringent test of the ability to calculate core electron correlation corrections than the S and P state lifetimes do. Correlation corrections in the S and P states are the dominant uncertainty in calculations of the $7S \leftrightarrow 8S$ parity nonconserving amplitude in francium [27]. The D states also present an interesting alternative for a parity nonconservation measurement [13].

ACKNOWLEDGMENTS

This work has been supported by the NSF. We thank C. T. Langlois for contributing to these measurements. We thank M. S. Safronova and W. R. Johnson for preliminary unpublished results, as well as V. A. Dzuba, V. V. Flambaum, and M. S. Safronova for helpful discussions.

[1] For a sample and overview of the extensive work performed at ISOLDE, see E. Arnold, W. Borchers, H.T. Duong, P. Juncar, J. Lermé, P. Lievens, W. Neu, R. Neugart, M. Pellarin, J. Pinard, J.L. Vialle, K. Wendt, and the ISOLDE Collaboration, J. Phys. B **23**, 3511 (1990).
[2] J.E. Simsarian, A. Ghosh, G. Gwinner, L.A. Orozco, G.D. Sprouse, and P.A. Voytas, Phys. Rev. Lett. **76**, 3522 (1996).
[3] Z.-T. Lu, K.L. Corwin, K.R. Vogel, C.E. Wieman, T.P. Dinneen, J. Maddi, and H. Gould, Phys. Rev. Lett. **79**, 994 (1997).
[4] J.E. Simsarian, L.A. Orozco, G.D. Sprouse, and W.Z. Zhao, Phys. Rev. A **57**, 2448 (1998).
[5] J.E. Simsarian, W.Z. Zhao, L.A. Orozco, and G.D. Sprouse, Phys. Rev. A **59**, 195 (1999).
[6] J.S. Grossman, L.A. Orozco, M.R. Pearson, J.E. Simsarian, G.D. Sprouse, and W.Z. Zhao, Phys. Rev. Lett. **83**, 935 (1999).
[7] V.A. Dzuba, V.V. Flambaum, and O.P. Sushkov, Phys. Rev. A **51**, 3454 (1995).
[8] M.S. Safronova, W.R. Johnson, and A. Derevianko, Phys. Rev. A **60**, 4476 (1999).
[9] M. S. Safronova and W. R. Johnson (private communication).
[10] J.E. Simsarian, S. Aubin, J.S. Grossman, L.A. Orozco, M.R. Pearson, G.D. Sprouse, and W.Z. Zhao, in *Parity Violations in Atoms and Polarized Electron Scattering*, edited by Bernard Frois and Marie-Anne Bouchiat (World Scientific, Singapore, 1999), p. 312.
[11] E. Arnold, W. Borchers, M. Carré, H.T. Duong, P. Juncar, J. Lermé, S. Liberman, W. Neu, R. Neugart, E.W. Otten, M. Pellarin, A. Pesnelle, J. Pinard, J.L. Vialle, K. Wendt, and the ISOLDE Collaboration, J. Phys. B **22**, L391 (1989).
[12] J.M. Grossman, R.P. Fliller III, T.E. Mehlstäubler, L.A. Orozco, M.R. Pearson, G.D. Sprouse, and W.Z. Zhao, Phys. Rev. A **62**, 052507 (2000).
[13] N. Fortson, Phys. Rev. Lett. **70**, 2383 (1993).
[14] G.D. Sprouse and L.A. Orozco, Annu. Rev. Nucl. Part. Sci. **47**, 429 (1997).
[15] D.V. O'Connor and D. Phillips, *Time Correlated Single Photon Counting* (Academic, London, 1984).
[16] L. Young, W.T. Hill III, S.J. Sibener, S.D. Price, C.E. Tanner, C.E. Wieman, and S.R. Leone, Phys. Rev. A **50**, 2174 (1994).
[17] B. Hoeling, J.R. Yeh, T. Takekoshi, and R.J. Knize, Opt. Lett. **21**, 74 (1996).
[18] R.G. DeVoe and R.G. Brewer, Opt. Lett. **19**, 1891 (1994).
[19] W.Z. Zhao, J.E. Simsarian, L.A. Orozco, and G.D. Sprouse, Rev. Sci. Instrum. **69**, 3737 (1998).
[20] W. Demtröder, *Laser Spectroscopy* (Springer-Verlag, Berlin, 1982).
[21] P. Schenck, R.C. Hilborn, and H. Metcalf, Phys. Rev. Lett. **31**, 189 (1973).
[22] W.A. van Wijngaarden and J. Xia, J. Quant. Spectrosc. Radiat. Transf. **61**, 557 (1999).
[23] E. Biémont, P. Quinet, and V. Van Renterghem, J. Phys. B **31**, 5301 (1998).
[24] C.E. Theodosiou, Bull. Am. Phys. Soc. **39**, 1210 (1994); (private communication, 1993).
[25] H.T. Duong, P. Juncar, S. Liberman, A.C. Mueller, R. Neugart, E.W. Otten, B. Peusse, J. Pinard, H.H. Stroke, C. Thibault, F. Touchard, J.L. Vialle, K. Wendt, and the ISOLDE Collaboration, Europhys. Lett. **3**, 175 (1987).
[26] V.A Dzuba (private communication); V.V. Flambaum (private communication).
[27] M.S. Safronova and W.R. Johnson, Phys. Rev. A **62**, 022112 (2000).